

## CATALYSIS

# Activation of surface lattice oxygen in single-atom Pt/CeO<sub>2</sub> for low-temperature CO oxidation

Lei Nie,<sup>1\*</sup> Donghai Mei,<sup>1\*</sup> Haifeng Xiong,<sup>2\*</sup> Bo Peng,<sup>1</sup> Zhibo Ren,<sup>1,3</sup> Xavier Isidro Pereira Hernandez,<sup>4</sup> Andrew DeLaRiva,<sup>2</sup> Meng Wang,<sup>1</sup> Mark H. Engelhard,<sup>1</sup> Libor Kovarik,<sup>1</sup> Abhaya K. Datye,<sup>2†</sup> Yong Wang<sup>1,4‡</sup>

To improve fuel efficiency, advanced combustion engines are being designed to minimize the amount of heat wasted in the exhaust. Hence, future generations of catalysts must perform at temperatures that are 100°C lower than current exhaust-treatment catalysts. Achieving low-temperature activity, while surviving the harsh conditions encountered at high engine loads, remains a formidable challenge. In this study, we demonstrate how atomically dispersed ionic platinum (Pt<sup>2+</sup>) on ceria (CeO<sub>2</sub>), which is already thermally stable, can be activated via steam treatment (at 750°C) to simultaneously achieve the goals of low-temperature carbon monoxide (CO) oxidation activity while providing outstanding hydrothermal stability. A new type of active site is created on CeO<sub>2</sub> in the vicinity of Pt<sup>2+</sup>, which provides the improved reactivity. These active sites are stable up to 800°C in oxidizing environments.

Advanced combustion engines are being developed to meet higher standards of fuel efficiency and lowered greenhouse gas emissions (1, 2), but their commercial potential is contingent on meeting emission standards for the control of criteria pollutants (CO, NO<sub>x</sub>, hydrocarbons, and particulate matter). The lower exhaust temperature of advanced engines requires catalysts that are active at temperatures <150°C to meet future emission regulations (3). Single-atom heterogeneous catalysts have demonstrated excellent low-temperature reactivity (4) but do not meet the demands of high-temperature thermal and/or hydrothermal durability that are needed during operation under high engine loads and periodic regeneration of catalytic soot filters.

We show that the activation of atomically dispersed Pt<sup>2+</sup> on CeO<sub>2</sub> via high-temperature (e.g., 750°C) treatment in steam simultaneously achieved the goals of low-temperature CO oxidation activity while providing thermal stability. Specifically, *T*<sub>100</sub> (temperature required to reach 100% conversion) of CO decreased from 320° to 148°C, and there was no evident catalyst deactivation in consecutive CO oxidation light-off measurements. In addition, cofeeding water further enhanced CO oxidation, and no detrimental

effects on CO oxidation by other pollutants, such as hydrocarbons and NO<sub>x</sub> present in the simulated vehicle exhaust, were observed—that is, *T*<sub>100</sub> of CO conversion was achieved at 150°C even under simulated exhaust conditions. The improved low-temperature activity is attributed to the activation of surface lattice oxygen that is bonded to H, forming hydroxyls on the CeO<sub>2</sub> support in the vicinity of atomically dispersed Pt. These results demonstrate the important role of activation of the catalyst support for simultaneously achieving high reactivity and durability, which remains a major challenge in the field of single-atom catalysis.

The oxidation of CO, a key reaction in automotive emission abatement, has been extensively studied (5–9). In the current generation of emission-treatment catalysts, the reaction is carried out over metallic nanoparticles (NPs) containing Pt, Pd, and Rh supported over aluminum oxide with other oxide promoters. Zero-valent atoms of platinum group metals (PGMs) are mobile at high temperatures and agglomerate into larger particles, losing their catalytic efficiency. To maintain this dispersion under working conditions, atoms must be anchored to the support by forming covalent bonds with oxygen atoms in the catalyst support. However, achieving high catalytic activity with anchored metal ions remains a formidable challenge.

A precious metal-based perovskite, LaFe<sub>0.95</sub>Pd<sub>0.05</sub>O<sub>3</sub>, was developed by Tanaka and co-workers (10) and termed the “intelligent” catalyst because of the ability of the precious metal to move in and out of perovskite oxides by forming a solid solution or metallic NP, depending on the redox conditions. In this manner, the sintering of the precious metal is prevented, but its low-temperature reactivity is limited. The U.S. Department of Energy has set the goal of achieving

90% conversion of all criteria pollutants at 150°C (“The 150°C Challenge”) (2), a temperature which is ~100°C lower than current state-of-the-art commercial automotive catalysts (11). In response to this challenge, the ternary oxide (without precious metals) CuCoCeO<sub>x</sub> was recently reported to outperform PGM-based catalysts in CO oxidation (12). However, its high-temperature hydrothermal stability limits its commercial deployment.

In this study, we used Pt and ceria (CeO<sub>2</sub>), which are two of the key components of catalytic converters in the market. Various efforts have been made to improve the dispersion of Pt to maximize its use (13–15). We recently reported that polyhedral CeO<sub>2</sub> can anchor Pt as isolated single atoms after thermal aging in air at 800°C to yield an atomically dispersed and sinter-resistant catalyst (7). However, despite its high dispersion and excellent thermal stability (5), the low-temperature CO oxidation reactivity is limited, partly due to the inactive lattice oxygen and strong binding of CO molecules to Pt ions (6).

The activity of ceria-supported catalysts can be improved by treating the catalyst in a reducing atmosphere (16), specifically in H<sub>2</sub>. However, such a reducing treatment causes the formation of Pt NPs (5, 9), which are subject to deactivation under oxidizing atmospheres (16). Surprisingly, we discovered that hydrothermal aging at high temperature (e.g., 750°C) can activate the atomically dispersed Pt/CeO<sub>2</sub> catalyst, leading to substantially improved low-temperature CO oxidation without any change in the atomic dispersion of Pt. Although steam treatment is widely used to improve catalytic stability of zeolites, it is rarely applied to supported PGM catalysts because sintering of the metal NPs and degradation of metal-oxide supports can occur (17, 18), leading to reduced catalyst activity.

We now show that steam treatment facilitated the formation of active surface lattice oxygen near atomically dispersed Pt and dramatically enhanced catalytic performance. We designated thermally aged and subsequently steam-treated (hydrothermally aged) catalysts as Pt/CeO<sub>2</sub> and Pt/CeO<sub>2</sub>-S, respectively. Catalyst preparation details are summarized elsewhere (fig. S1) (19). In the Pt/CeO<sub>2</sub> catalyst (Fig. 1A), Pt is atomically dispersed, in agreement with our previous report (7). Interestingly, in the Pt/CeO<sub>2</sub>-S sample, no sintering of Pt occurred, and Pt remained atomically dispersed (Fig. 1B), even after harsh steam treatment at the high temperature of 750°C. The presence of Pt NPs should be readily visible by scanning transmission electron microscopy (STEM) (fig. S2). No such NPs were found in Pt/CeO<sub>2</sub> or Pt/CeO<sub>2</sub>-S, even by higher-resolution STEM. No diffraction peaks of Pt were observed in x-ray diffraction patterns for both Pt/CeO<sub>2</sub> and Pt/CeO<sub>2</sub>-S samples, further confirming the high dispersion of Pt (fig. S3). The x-ray absorption near-edge structure spectra show that the Pt remained oxidized on both Pt/CeO<sub>2</sub> and Pt/CeO<sub>2</sub>-S samples and that there were no detectable Pt–Pt first- or second-shell interactions in the extended x-ray absorption fine structure (EXAFS) results, verifying the atomic dispersion

<sup>1</sup>Institute for Integrated Catalysis and Environmental Molecular Sciences Laboratory, Pacific Northwest National Laboratory, Post Office Box 999, Richland, WA 99352, USA.

<sup>2</sup>Department of Chemical and Biological Engineering and Center for Micro-Engineered Materials, University of New Mexico, Albuquerque, NM 87131, USA. <sup>3</sup>State Key Laboratory of Chemical Resources Engineering, Beijing University of Chemical Technology, Beijing 100029, China. <sup>4</sup>The Gene and Linda Voiland School of Chemical Engineering and Bioengineering, Washington State University, Pullman, WA 99164, USA.

\*These authors contributed equally to this work.

†Corresponding author. Email: datye@unm.edu (A.K.D.); yong.wang@pnl.gov (Y.W.)

of Pt (fig. S4). Moreover, the surface areas and pore volumes for Pt/CeO<sub>2</sub> and Pt/CeO<sub>2</sub>\_S were comparable to each other (table S1), suggesting the existence of stable textural properties after high-temperature steam treatment. Additionally, Pt remained in ionic form Pt<sup>2+</sup> over both catalysts, as evidenced by x-ray photoelectron spectroscopy (XPS) (fig. S5).

It is generally accepted that the CO oxidation over Pt/CeO<sub>2</sub> follows a Mars-van Krevelen reaction mechanism, (13, 20). Adsorbed CO on Pt reacts with active lattice oxygen species provided by CeO<sub>2</sub>, where no competitive adsorption between CO and O<sub>2</sub> is involved. The reaction rates do not depend on the partial pressure of both CO and O<sub>2</sub>, i.e., 0<sup>th</sup> order (8, 27). The reaction mechanism and kinetics are valid over a wide range of reactant compositions (lean, stoichiometric, and rich conditions) (20).

To mimic lean-burn diesel engine exhaust, we used excess O<sub>2</sub> in the reactant (CO/O<sub>2</sub> = 1/25 in molar ratio) (12). The CO oxidation light-off curves were measured to evaluate catalyst performance. A gas hourly space velocity of 200,000 ml g<sub>cat</sub><sup>-1</sup> hour<sup>-1</sup> (g<sub>cat</sub>, grams of catalyst) was used to match standard vehicle exhaust conditions. As shown in Fig. 1C, Pt/CeO<sub>2</sub> showed a high onset temperature of ~210°C. After steam treatment (hydrothermal aging) at 750°C, the Pt/CeO<sub>2</sub>\_S exhibited dramatically improved low-temperature reactivity, compared to that of Pt/CeO<sub>2</sub>, as the onset

temperature was lowered to ~60°C, and T<sub>100</sub> decreased from 320° (Pt/CeO<sub>2</sub>) to 148°C (Pt/CeO<sub>2</sub>\_S).

Compared to other reported catalysts that have potential commercial viability as well as current commercial catalysts tested under similar conditions that have been subjected to 800°C treatment in air, Pt/CeO<sub>2</sub>\_S is among the most active CO oxidation catalysts (table S2). Because the Pt/CeO<sub>2</sub>\_S catalyst was pretreated under harsh hydrothermal conditions at 750°C, it is not surprising that it also exhibits stable reactivity. There is no noticeable deactivation during 310-hour time-on-stream testing with eight light-off cycles, and 95% conversion of CO is maintained at 145°C for 310 hours (fig. S6).

For comparison, we also tested CoCuCeO<sub>x</sub> and 0.5% Pd/La-Al<sub>2</sub>O<sub>3</sub>, which are two other promising catalysts (table S2) (12, 22). After hydrothermal aging under the same conditions as the Pt/CeO<sub>2</sub>\_S catalyst, their T<sub>100</sub> increased to 350° and 190°C, respectively (Fig. 1D). To further investigate the durability of Pt/CeO<sub>2</sub>\_S especially at high temperatures, which is crucial for operations under high engine loads, light-off performance at temperatures up to 500° and 800°C was tested (fig. S7). No evident deactivation was found at 500°C (fig. S7A), and slight deactivation was observed at 800°C after one cycle, but stable performance was maintained thereafter (fig. S7B). Furthermore, there is no detrimental effect on CO oxidation by other pollutants, such

as hydrocarbons and NO<sub>x</sub>, in the feed when the CO oxidation performance of Pt/CeO<sub>2</sub>\_S was evaluated under simulated exhaust conditions (fig. S8A). In addition, cofeeding water could further enhance the low-temperature CO oxidation activity over Pt/CeO<sub>2</sub>\_S (fig. S8B), as previously reported (13).

To provide mechanistic insights into the enhanced low-temperature CO oxidation reactivity of Pt/CeO<sub>2</sub> by steam treatment, adsorption of CO over Pt sites was studied by diffuse-reflectance infrared Fourier-transform spectroscopy (DRIFTS) for both Pt/CeO<sub>2</sub> and Pt/CeO<sub>2</sub>\_S catalysts (6). Under CO oxidation reaction conditions at 180°C (CO oxidation steady state in Fig. 2, A and B), only ionic Pt<sup>2+</sup> was present, as evidenced by the bands at 2096 and 2098 cm<sup>-1</sup>, which are assigned to linearly adsorbed CO on isolated ionic Pt<sup>2+</sup> (6, 23). By combining the results from STEM (Fig. 1, A and B), XPS (fig. S5), DRIFTS, and EXAFS (fig. S4), we conclude that atomic dispersion of Pt<sup>2+</sup> was maintained on both Pt/CeO<sub>2</sub>\_S and Pt/CeO<sub>2</sub> and that steam treatment did not affect the dispersion or valence (Pt<sup>2+</sup>) of platinum.

Over Pt/CeO<sub>2</sub>, the infrared (IR) band (2098 cm<sup>-1</sup>) did not change appreciably after CO flow was stopped at 180°C while O<sub>2</sub> continued to flow (Fig. 2A). This result suggested that CO adsorption on the ionic Pt site was very strong at 180°C, as reported previously (6, 7), and it is consistent with the lack of activity for Pt/CeO<sub>2</sub> below 210°C (Fig. 1C). However, over Pt/CeO<sub>2</sub>\_S, after CO flow was discontinued for 15 min at 180°C (with continuing O<sub>2</sub> flow), the intensity of the IR band at 2096 cm<sup>-1</sup> decreased substantially (by 57%) (Fig. 2B) as opposed to a 7% reduction on Pt/CeO<sub>2</sub> (Fig. 2A), suggesting that the CO adsorbed on single-ion Pt<sup>2+</sup> was readily oxidized to CO<sub>2</sub>.

This observation agrees well with the low-temperature CO oxidation reactivity shown in Fig. 1C, i.e., Pt/CeO<sub>2</sub>\_S became active at 60°C and 100% conversion was achieved at 148°C. We concluded that CO adsorbed on Pt<sup>2+</sup> in the Pt/CeO<sub>2</sub>\_S sample was more reactive than that adsorbed on Pt<sup>2+</sup> in the Pt/CeO<sub>2</sub> sample. Because Pt on both samples Pt/CeO<sub>2</sub>\_S and Pt/CeO<sub>2</sub> exhibited the same atomic dispersion and valence (Pt<sup>2+</sup>), the difference in low-temperature reactivity between Pt/CeO<sub>2</sub>\_S and Pt/CeO<sub>2</sub> could be attributed to neighboring lattice oxygen, which is part of the active site (6, 9, 24) and thus should have a dramatic effect on the reactivity of the ionic Pt sites.

Active lattice oxygen, usually associated with the oxygen vacancies on the uppermost ceria layers in vicinity of Pt sites, can be considered to be part of the active sites for this reaction. However, they are short-lived and are difficult to observe under steady-state reaction conditions because the reoxidation rate of oxygen vacancies is at least one order of magnitude faster than that of oxygen-vacancy generation (20, 25). Hence, CO<sub>2</sub> formation in time-resolved CO oxidation experiments was used to semiquantitatively measure these short-lived active oxygen species at 300°C. Compared to the Pt/CeO<sub>2</sub> sample, steam

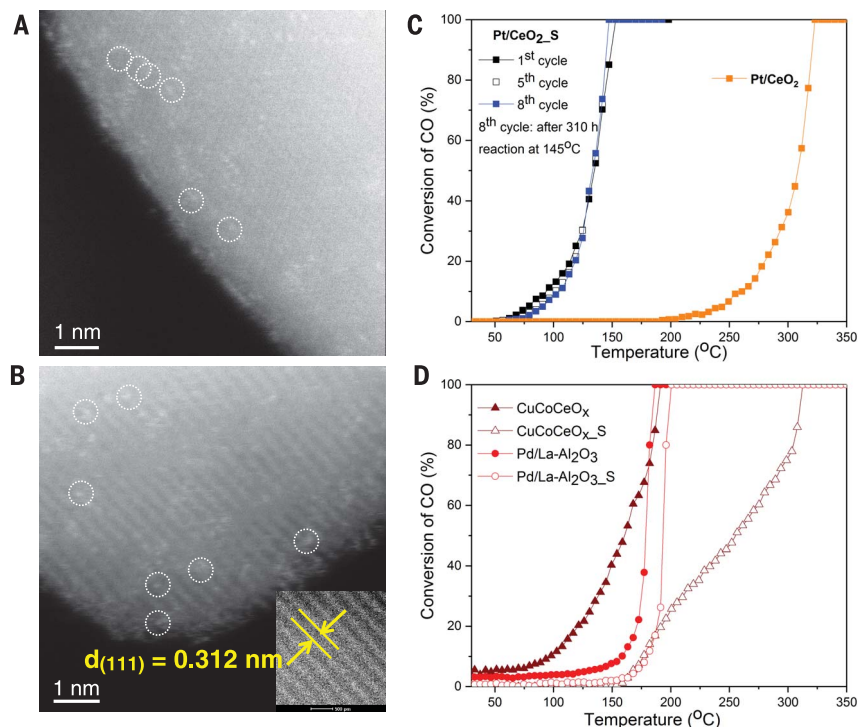


**Fig. 1. Characterization and performance of Pt/CeO<sub>2</sub> catalysts.** Representative aberration-corrected-STEM images of (A) Pt/CeO<sub>2</sub> and (B) Pt/CeO<sub>2</sub>\_S. Single atoms of Pt are circled in the images.  $d_{(111)}$ , CeO<sub>2</sub>(111) lattice spacing. (C and D) Catalytic CO oxidation light-off performance of different catalysts. [O<sub>2</sub>] = 10% and [CO] = 0.4% balanced with argon at a gas hourly space velocity of 200,000 ml g<sub>cat</sub><sup>-1</sup> hour<sup>-1</sup>. Temperature ramp, 2°C per min; pressure, 1 atm.

treatment roughly doubled the amount of active lattice oxygen in Pt/CeO<sub>2</sub>\_S (Fig. 2C).

The oxygen species of the catalysts were further characterized by H<sub>2</sub> temperature-programmed reduction (H<sub>2</sub>-TPR) analysis (Fig. 2D). The reduction of bulk oxygen on CeO<sub>2</sub> took place at or above 600°C, and the absence of reduction peak below room temperature was confirmed by cryogenic H<sub>2</sub>-TPR (5). Two major reduction peaks were observed for the Pt/CeO<sub>2</sub> sample: (i) reduction of the surface lattice oxygen in the vicinity of Pt (Pt–O–Ce bond), centered at 184°C; and (ii) reduction of surface lattice oxygen on CeO<sub>2</sub> distant from Pt, centered at 348°C (5, 24). Over Pt/CeO<sub>2</sub>\_S, an extra peak at 162°C was observed, which was likely caused by a new type of active surface lattice oxygen generated during steam treatment. It is possible that over Pt/CeO<sub>2</sub>\_S, CO adsorbed on Pt sites was readily oxidized by this type of active surface lattice oxygen, as confirmed by DRIFTS (Fig. 2B), but over Pt/CeO<sub>2</sub>, it was not (Fig. 2A). Detailed quantitative analysis for H<sub>2</sub>-TPR (fig. S9) suggests that some of the surface oxygen on CeO<sub>2</sub> near Pt was also reduced by H<sub>2</sub> at a temperature <200°C in addition to the Pt–O–Ce bonds (and/or the activated surface lattice oxygen).

It has been accepted that the CO oxidation reaction over metallic Pt supported on nonreducible oxides (Al<sub>2</sub>O<sub>3</sub>, SiO<sub>2</sub>, etc.) follows a Langmuir-Hinshelwood mechanism. For example (26, 27), over Pt/Al<sub>2</sub>O<sub>3</sub>, CO has an inhibiting effect on Pt<sup>0</sup> reactivity at low temperatures due to competitive adsorption between CO and O<sub>2</sub>, with a rate inversely proportional to the partial pressure of CO and first-order proportional to O<sub>2</sub>. By contrast, over Pt/CeO<sub>2</sub> catalysts, a Mars-van Krevelen reaction mechanism is followed by dissociative O<sub>2</sub> adsorption and activation, preferentially occurring on ceria (in the vicinity of Pt), and the competitive adsorption between O<sub>2</sub> and CO over the metal sites is circumvented (8, 20, 21). Both Pt/CeO<sub>2</sub> and Pt/CeO<sub>2</sub>\_S have similar atomically dispersed Pt in the form of Pt<sup>2+</sup>, so the active surface lattice oxygen aforementioned should be responsible for the differences in the low-temperature reactivity of these two catalysts.

In the current study, the Pt/CeO<sub>2</sub> sample (aged in air at 800°C) did not show CO oxidation activity at temperatures lower than 210°C (Fig. 1C). It was reported that thermal aging at 800°C led to strong Pt–O–Ce bond formation (5), which over stabilizes the surface lattice oxygen and results in the lack of low-temperature CO oxidation reactivity (24). However, the strong Pt–O–Ce bond led to atomically dispersed Pt and excellent thermal stability (without Pt sintering or CeO<sub>2</sub> structure collapse). For Pt/CeO<sub>2</sub>\_S, the Pt–O–Ce bond was retained even after harsh steam treatment (i.e., Pt remained as atomically dispersed), which was also evidenced by the XPS and Raman spectra (figs. S5 and S10). Thus, compared to Pt/CeO<sub>2</sub>, the improvement in low-temperature CO oxidation reactivity of Pt/CeO<sub>2</sub>\_S could be attributed to the effect of high-temperature steam treatment (H<sub>2</sub>O vapor), whose role is complex.

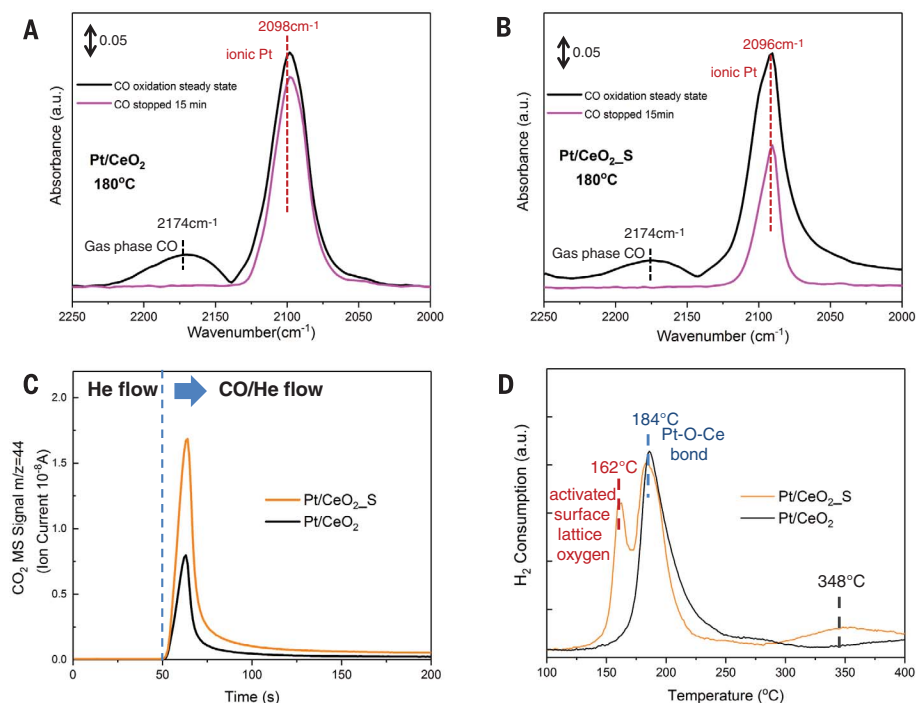


**Fig. 2. Identification of Pt single atoms (Pt<sup>2+</sup>) and active surface lattice oxygen.** CO adsorption DRIFTS for (A) Pt/CeO<sub>2</sub> and (B) Pt/CeO<sub>2</sub>\_S. After 30 min of CO oxidation (black lines), the CO flow was discontinued, and the recording of spectra continued for 15 min with continuing O<sub>2</sub> flow (magenta lines). Temperature, 180°C; a.u., arbitrary units. (C) Time-resolved CO oxidation with surface active lattice oxygen of Pt/CeO<sub>2</sub> catalysts at 300°C. Conditions: 50 standard cubic centimeter per minute (SCCM) of He from 0 to 50 s; 50 SCCM of 10% CO in He from 50 to 200 s. (D) H<sub>2</sub>-TPR profiles of Pt/CeO<sub>2</sub> catalysts.

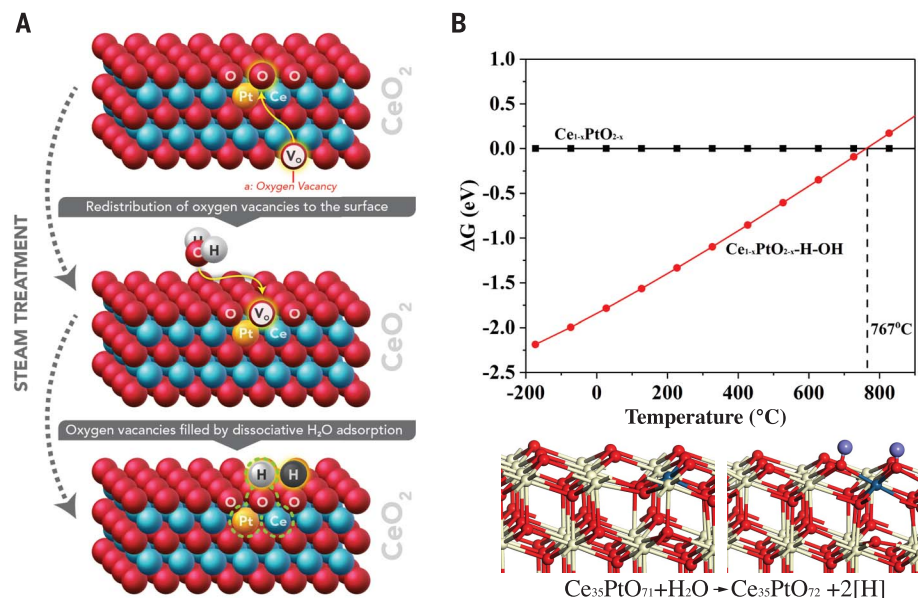


**Fig. 3. Illustration of steam-treatment effects on the atomically dispersed Pt/CeO<sub>2</sub> catalyst.** (A) The active site created by the steam treatment, which is responsible for low-temperature CO oxidation activity, is highlighted by dashed green circles. (B) Gibbs free energy ( $\Delta G^\circ$ ) of dissociative water adsorption on the atomically dispersed Pt/CeO<sub>2</sub> surface. One oxygen vacancy was filled by water under steam-treatment conditions ( $P_{\text{H}_2\text{O}} = 0.1$  atm).

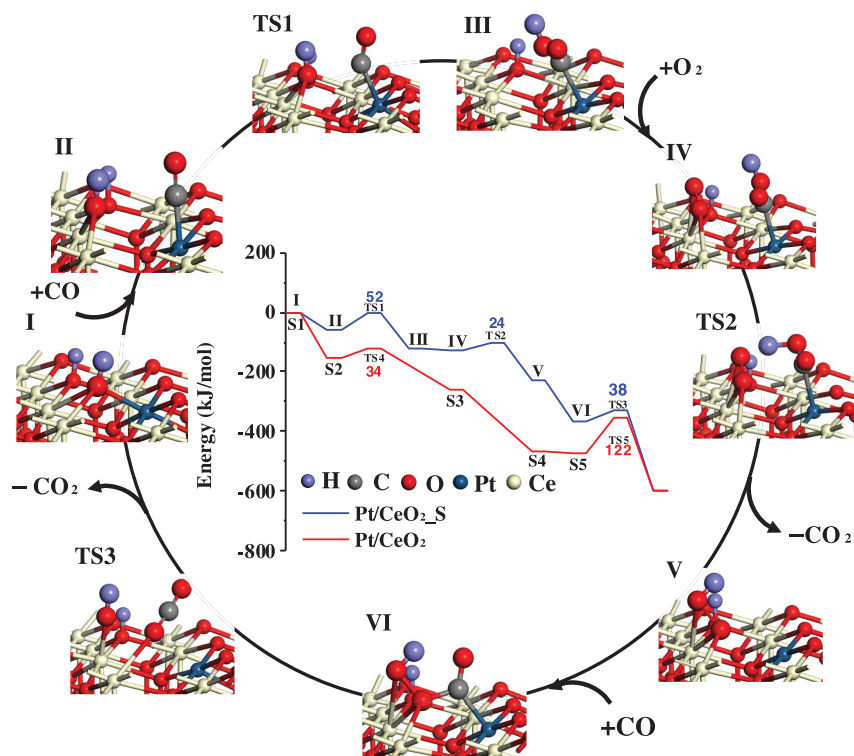


**Fig. 4. Proposed reaction mechanism for CO oxidation on isolated Pt on a CeO<sub>2</sub>(111) surface.**

The inset shows the calculated energy profiles in kJ mol<sup>-1</sup>. The structures of intermediates and transition states (TSs) of the key elementary steps are shown in the reaction cycle. The reaction cycle corresponds to the energy profile for Pt/CeO<sub>2</sub>\_S (steam-treated Pt/CeO<sub>2</sub>), which is shown by the blue line in the inset. The red line shows the energy profile for Pt/CeO<sub>2</sub> (reaction cycle is shown in fig. S12).

To better understand the nature of this new type of active surface lattice oxygen generated by high-temperature steam treatment (H<sub>2</sub>O vapor) on atomically dispersed Pt/CeO<sub>2</sub>, density functional theory calculations and reaction kinetic analyses were conducted. Oxygen vacancies from the CeO<sub>2</sub> bulk can be redistributed to the CeO<sub>2</sub>(111) surface (Fig. 3A) as a result of exposure to water at a high temperature of 380°C, as previously reported (28). Under steam-treatment conditions, H<sub>2</sub>O molecules can then fill out the oxygen vacancy (V<sub>O</sub>) over the atomically dispersed Pt/CeO<sub>2</sub> surface, generating two neighboring active O<sub>lattice</sub>[H] in the vicinity of Pt (Fig. 3A), which are thermodynamically stable up to 767°C (Fig. 3B).

Accordingly, the CO oxidation reaction cycle over this steam-treated atomically dispersed Pt/CeO<sub>2</sub>\_S was considered. The calculated energy profile is shown in Fig. 4 (inset, blue line), with detailed results summarized (table S3). The starting configuration only involves one catalytically active O<sub>lattice</sub>[H] site, coordinated with a Pt atom (Pt<sup>2+</sup>) (Fig. 4, intermediate I). The surface O<sub>lattice</sub>[H] reacts with CO adsorbed on Pt and creates an V<sub>O</sub> (Fig. 4, intermediate III) with an activation barrier of 52 kJ mol<sup>-1</sup> and exothermicity ( $\Delta H$ ) of -63 kJ mol<sup>-1</sup>. The V<sub>O</sub> is then filled by adsorption of an oxygen molecule. CO<sub>2</sub> is generated via the deprotonation of the carboxyl intermediate assisted by the newly adsorbed oxygen molecule

with an activation barrier of 24 kJ mol<sup>-1</sup> [(Fig. 4, transition state 2 (TS2)]. Thereafter, the OO[H] species (Fig. 4, intermediate V) reacts with the second adsorbed CO, generating another CO<sub>2</sub> molecule with a smaller activation barrier of 38 kJ mol<sup>-1</sup> (Fig. 4, TS3). Finally, the atomically dispersed Pt/CeO<sub>2</sub>\_S surface is recovered after CO<sub>2</sub> desorption, and the catalytic cycle over the steam-treated catalyst surface (2O<sub>lattice</sub>[H]) is closed. The overall energy barrier of the entire reaction cycle is 52 kJ mol<sup>-1</sup>, which is in agreement with the measured apparent activation energy from the Arrhenius plot of 43 kJ mol<sup>-1</sup> for atomically dispersed Pt/CeO<sub>2</sub>\_S (fig. S11).

For comparison, CO oxidation over Pt/CeO<sub>2</sub> without steam treatment was also calculated (Fig. 4; inset, red line). In this case, the reaction cycle starts with the reaction of CO with the adsorbed O<sub>2</sub> at the V<sub>O</sub> site (fig. S12, TS4). After CO<sub>2</sub> desorption, the surface V<sub>O</sub> is filled as the O<sub>lattice</sub>. Then, the O<sub>lattice</sub> reacts with the second adsorbed CO at the Pt site, forming the second CO<sub>2</sub> (fig. S12, TS5). The overall activation barrier is 122 kJ mol<sup>-1</sup>, which, again, agrees with the apparent activation energy of 105 kJ mol<sup>-1</sup> for Pt/CeO<sub>2</sub> (fig. S11), more than double that of Pt/CeO<sub>2</sub>\_S.

The active O<sub>lattice</sub>[H] site generated from steam treatment is fundamentally different from the previously reported surface OH on the Ce that is

formed over atomically dispersed Pt/CeO<sub>2</sub> by co-feeding water during CO oxidation (13) or water dissociation over Pt/CeO<sub>2</sub> (29–32). Co-feeding water in the reactants can further enhance the low-temperature CO oxidation activity over Pt/CeO<sub>2</sub>\_S (fig. S8B). However, such enhancement disappeared when water in the feed was discontinued, because of the instability of the OH groups formed on the Ce under reaction conditions (13). By contrast, here, the active O<sub>lattice</sub>[H] generated via high-temperature steam treatment is thermally much more stable (up to 767°C), and below this temperature, it can be readily regenerated during CO oxidation reaction cycles without the need to co-feed water. This difference is the main reason that we observed no deactivation during light-off measurements up to 500°C (fig. S7A), and only at 800°C did we see slight deactivation of the catalyst (fig. S7B). This is further confirmed by the fact that all Pt remains as single atoms after the first cycle to 800°C, as evidenced by aberration-corrected-STEM (fig. S13). The stronger basicity of the O<sub>lattice</sub>[H] compared to that of surface OH may also lead to the optimal Lewis acid-base pairs that promote low-temperature CO oxidation.

Water vapor is always present in vehicle exhaust, and thus, our catalyst would be inherently stable under exhaust conditions because it was synthesized via calcination at 800°C in air followed by steam treatment at 750°C. More importantly, this enhanced CO oxidation is also found to occur on other commercially available ceria, for example, from Aldrich and Rhodia (figs. S14 and S15). High-temperature steam treatment not only enhances CO oxidation under simulated vehicle exhaust conditions (fig. S16A), but also improves the oxidation of other components of exhaust, such as saturated and unsaturated hydrocarbons (propane and propylene) and NO<sub>x</sub> (figs. S16, B and C, and S17). The enhanced reactivity is not the result of the formation of Pt NPs, but rather the activation of surface oxygen on the ceria support. This demonstration of hydrothermal stability, along with high reactivity, makes it possible to bring single-atom catalysis closer to industrial application.

#### REFERENCES AND NOTES

1. Chemical Sciences Roundtable, Board on Chemical Sciences and Technology, National Research Council, "Carbon Management: Implications for R&D in the Chemical Sciences and Technology" (Workshop Report, Chemical Sciences Roundtable, 2001), pp. 93–110.
2. M. Zammit et al., "Future automotive aftertreatment solutions: The 150°C Challenge workshop report," (U.S. DRIVE Report, Southfield, MI, 2013).
3. National Archives and Records Administration, *Fed. Regist.* **81**, 73478–74274 (2016).
4. X.-F. Yang et al., *Acc. Chem. Res.* **46**, 1740–1748 (2013).
5. J. Lee, Y. S. Ryou, X. Chan, T. J. Kim, D. H. Kim, *J. Phys. Chem. C* **120**, 25870–25879 (2016).
6. K. Ding et al., *Science* **350**, 189–192 (2015).
7. J. Jones et al., *Science* **353**, 150–154 (2016).
8. M. Cargnello et al., *Science* **341**, 771–773 (2013).
9. S. Gatta et al., *ACS Catal.* **6**, 6151–6155 (2016).
10. Y. Nishihata et al., *Nature* **418**, 164–167 (2002).
11. H.-L. Chang, H.-Y. Chen, K. Koo, J. Rieck, P. Blakeman, *SAE Int. J. Fuel Lubr.* **7**, 480–488 (2014).
12. A. J. Binder, T. J. Toops, R. R. Unocic, J. E. Parks II, S. Dai, *Angew. Chem. Int. Ed.* **54**, 13263–13267 (2015).

13. C. Wang *et al.*, *ACS Catal.* **7**, 887–891 (2017).
14. F. Dvořák *et al.*, *Nat. Commun.* **7**, 10801 (2016).
15. A. Bruix *et al.*, *Angew. Chem. Int. Ed.* **53**, 10525–10530 (2014).
16. J. G. Nunan, H. J. Robota, M. J. Cohn, S. A. Bradley, *J. Catal.* **133**, 309–324 (1992).
17. S. Balcon, S. Mary, C. Kappenstein, E. Gengembre, *Appl. Catal. A Gen.* **196**, 179–190 (2000).
18. S. J. Schmieg, D. N. Belton, *Appl. Catal. B* **6**, 127–144 (1995).
19. See supplementary materials.
20. R. Kopelent *et al.*, *Angew. Chem.* **127**, 8852–8855 (2015).
21. H.-H. Liu *et al.*, *Appl. Surf. Sci.* **314**, 725–734 (2014).
22. E. J. Peterson *et al.*, *Nat. Commun.* **5**, 4885 (2014).
23. P. Bazin, O. Saur, J. Lavalley, M. Daturi, G. Blanchard, *Phys. Chem. Chem. Phys.* **7**, 187–194 (2005).
24. J. Ke *et al.*, *ACS Catal.* **5**, 5164–5173 (2015).
25. L. Artiglia *et al.*, *J. Phys. Chem. Lett.* **8**, 102–108 (2017).
26. A. D. Allian *et al.*, *J. Am. Chem. Soc.* **133**, 4498–4517 (2011).
27. M. Chen *et al.*, *Surf. Sci.* **601**, 5326–5331 (2007).
28. M. A. Henderson, C. Perkins, M. H. Engelhard, S. Thevuthasan, C. H. Peden, *Surf. Sci.* **526**, 1–18 (2003).
29. Y. Lykhach *et al.*, *J. Phys. Chem. C* **116**, 12103–12113 (2012).
30. D. R. Mullins *et al.*, *J. Phys. Chem. C* **116**, 19419–19428 (2012).
31. M. Molinari, S. C. Parker, D. C. Sayle, M. S. Islam, *J. Phys. Chem. C* **116**, 7073–7082 (2012).
32. A. Bruix *et al.*, *J. Am. Chem. Soc.* **134**, 8968–8974 (2012).

#### ACKNOWLEDGMENTS

This work was primarily supported by the U.S. Department of Energy (DOE), Office of Science, Basic Energy Sciences (BES) and Division of Chemical Sciences (grant DE-FG02-05ER15712). Additional support from the DOE, Office of Energy Efficiency and Renewable Energy, Vehicle Technology Office, and the Pacific Northwest National Laboratory (PNNL) Laboratory Directed Research and Development Materials Synthesis and Simulation Across Scales Initiatives (L.N.); and DOE Office of Science BES under DE-AC05-RL01830 and FWP-47319 (Z.R. and D.M.) is acknowledged. Catalyst characterization was primarily performed at the Environmental Molecular Sciences Laboratory, a DOE Office of Science User Facility sponsored by the Office of Biological and

Environmental Research, located at PNNL. PNNL is operated for DOE by Battelle. Use of the Advanced Photon Source, an Office of Science User Facility operated for the DOE Office of Science by Argonne National Laboratory, was supported by the DOE under contract no. DE-AC02-06CH11357. We also thank H. Shi for discussions and comments on the manuscript. All data are reported in the main text and supplementary materials. Certain aspects of the paper are described in U.S. patent application 62/579,959.

#### SUPPLEMENTARY MATERIALS

[www.sciencemag.org/content/358/6369/1419/suppl/DC1](http://www.sciencemag.org/content/358/6369/1419/suppl/DC1)  
Materials and Methods  
Supplementary Text  
Figs. S1 to S18  
Tables S1 to S4  
References (33–38)

26 June 2017; resubmitted 6 September 2017  
Accepted 13 November 2017  
10.1126/science.aao2109

## Activation of surface lattice oxygen in single-atom Pt/CeO<sub>2</sub> for low-temperature CO oxidation

Lei Nie, Donghai Mei, Haifeng Xiong, Bo Peng, Zhibo Ren, Xavier Isidro Pereira Hernandez, Andrew DeLaRiva, Meng Wang, Mark H. Engelhard, Libor Kovarik, Abhaya K. Datye and Yong Wang

*Science* **358** (6369), 1419-1423.  
DOI: 10.1126/science.aao2109

### Stable catalysts through steaming

The lifetime of catalysts that convert automotive exhaust pollutants can be increased by lowering their operating temperature, which helps to prevent deactivation caused by the active metal atoms agglomerating into larger, less active particles. Nie *et al.* show that a thermally stable catalyst, atomically dispersed Pt<sup>2+</sup> on CeO<sub>2</sub>, can become active for CO oxidation at 150°C after steam treatment at 750°C. In studies with simulated vehicle exhaust, this catalyst treatment also improves its oxidation activity for other exhaust components such as hydrocarbons.

*Science*, this issue p. 1419

#### ARTICLE TOOLS

<http://science.sciencemag.org/content/358/6369/1419>

#### SUPPLEMENTARY MATERIALS

<http://science.sciencemag.org/content/suppl/2017/12/13/358.6369.1419.DC1>

#### REFERENCES

This article cites 35 articles, 3 of which you can access for free  
<http://science.sciencemag.org/content/358/6369/1419#BIBL>

#### PERMISSIONS

<http://www.sciencemag.org/help/reprints-and-permissions>

Use of this article is subject to the [Terms of Service](#)